Effects of strain on the electron effective mass in GaN and AlN

C. E. Dreyer, A. Janotti, and C. G. Van de Walle
Materials Department, University of California, Santa Barbara, California 93106-5050, USA

(Received 30 January 2013; accepted 27 March 2013; published online 10 April 2013)

Stress is known to strongly alter the effective mass in semiconductors, changing the mobility of carriers. Transport measurements on AlGaN/GaN heterostructures indicated a large increase in mobility under tensile strain [M. Azize and T. Palacios, J. Appl. Phys. **108**, 023707 (2010)]. Using first-principles methods, we calculate the variation of electron effective mass in GaN and AlN under hydrostatic and biaxial stress. Unexpected trends are found, which are explained within $\mathbf{k}\cdot\mathbf{p}$ theory through a variation of the interband momentum matrix elements. The magnitude of the effective-mass reduction is too small to explain the experimentally reported increase in mobility.
© *2013 AIP Publishing LLC*. [http://dx.doi.org/10.1063/1.4801520]

The electronic and transport properties of semiconductors can be significantly altered by applying stress. Carrier-mobility enhancement with strain is well characterized in Si, and this effect is exploited in the design of Si-based transistors.[1] Recent experiments on high electron mobility transistors (HEMTs) based on AlGaN/GaN heterostructures indicate an increase of 25% in sheet electron density, and an enhancement as large as 20% in the electron mobility with 0.16% tensile strain under applied biaxial stress.[2] The authors speculated that the increase in mobility resulted from a decrease in the electron effective mass due to strain. This hypothesis motivated us to examine the variation of electron effective mass with strain in GaN and AlN by performing state-of-the-art first-principles calculations.

The effects of biaxial and hydrostatic stress on the band gap and valence-band structure of III-nitrides have been thoroughly investigated, but effects of stress on electron effective mass have been scarcely explored. Gorczyca *et al.*[3] used density functional theory (DFT) to study the variation of effective mass with hydrostatic pressure in InN. Svane *et al.*[4] used quasiparticle calculations for GaN, but again focused only on hydrostatic pressure.

Our present calculations are based on DFT using the screened hybrid functional of Heyd, Scuseria, and Ernzerhof (HSE),[5,6] which provides a much more accurate description of the electronic structure than traditional functionals. We also provide an interpretation of our results in the context of $\mathbf{k}\cdot\mathbf{p}$ theory, and show that the variation of the interband momentum matrix elements with strain needs to be taken into account to produce accurate trends. Our approach illustrates the power of combining first-principles DFT calculations with semi-empirical $\mathbf{k}\cdot\mathbf{p}$ modeling.

The DFT-HSE calculations are performed using the VASP code,[7] implemented with projector augmented wave (PAW) potentials.[8] The Ga *d* electrons were frozen in the core of the pseudopotential. Tests including the Ga *d* electrons in the valence indicate that our conclusions remain unaffected. The hybrid functional approach produces accurate band structures and correctly captures the effects of strain on the band structure of nitrides.[9] We have found that it also produces equilibrium effective mass in good agreement with experiment[10] and with quasiparticle G_0W_0 calculations[11] (see Table I). We use an energy cutoff of 600 eV for the plane-wave basis set, a mixing parameter of 31% (percentage of Hartree-Fock exchange in the exchange-correlation functional), and a mesh of $6\times6\times4$ special **k**-points for the integrations over the Brillouin zone of the wurtzite primitive cell. The calculated band gaps and lattice constants are in good agreement with experimental values.[12]

We have studied the variation of the band gap and electron effective mass in GaN and AlN under both hydrostatic and in-plane (i.e., perpendicular to the *c* direction) biaxial stress. We approximate hydrostatic stress by imposing hydrostatic *strain*, i.e., changing the lattice parameters of the wurtzite cell equally ($\epsilon_{xx}=\epsilon_{yy}=\epsilon_{zz}$) and allowing the internal structural *u* parameter to fully relax. The *c*/*a* ratio of the wurtzite structure slightly decreases with increasing hydrostatic stress,[13] but the effect on the band gap is negligibly small for the relatively small strains considered here.[3] For the case of biaxial stress, the in-plane lattice parameters were changed equally, and the crystal was allowed to relax in the *c* direction ($\epsilon_{xx}=\epsilon_{yy}\neq\epsilon_{zz}$). In this configuration, the macroscopic theory of elasticity predicts that the strains should be related by $\epsilon_{zz}=-2(C_{13}/C_{33})\epsilon_{xx}$. Our calculated values of $-2C_{13}/C_{33}$ (-0.564 for GaN and -0.571 for AlN) are within the range of reported experimental values[10] (-0.369 to -0.684 for GaN and -0.509 to -0.606 for AlN).

We determined the electron effective mass by analyzing the calculated band structure near Γ along the A direction in reciprocal space ($m_e^{\parallel}$, parallel to the *c* direction of the crystal) and along the M and K directions ($m_e^{\perp}$, perpendicular to the *c* direction), as indicated in Fig. 1. We found the electron effective mass in the M and K directions to be equal at zero strain and to remain equal under the stress states explored here.

Figure 2 displays our results for the variation of band gap under imposed strain. Hydrostatic stress causes the band gap to increase linearly under compression, with a deformation potential $a_g=dE_g/d\ln V$ of -8.31 eV for GaN and -9.88 eV for AlN. These values fall within the range of reported experimental[10] and theoretical[14] hydrostatic deformation potentials: -7.8 to -11.8 eV for GaN and -7.1 to -11.8 eV for AlN.[10]

For biaxial stress, the band gap also increases with compression, but the ordering of the topmost valence-band states

 © 2013 AIP Publishing LLC

TABLE I. Equilibrium (zero-strain) electron effective mass parallel and perpendicular to the c direction in units of free electron mass compared to selected literature values.

	Direction	Experiment (Ref. 10)	G_0W_0 (Ref. 11)	HSE (this work)
GaN	$m_e^{\parallel}$	0.18–0.29	0.19	0.19
	$m_e^{\perp}$	0.18–0.29	0.21	0.22
AlN	$m_e^{\parallel}$	0.29–0.45	0.32	0.30
	$m_e^{\perp}$	0.29–0.45	0.33	0.32

is now affected. The relevant valence bands near Γ, denoted by their symmetry character,[15] are the heavy hole, HH (Γ_9) and light hole, LH (Γ_7) bands, and the crystal-field split-off band, CF (Γ_7). The HH and LH bands are degenerate because spin-orbit interaction (which is very small in the nitrides, 17.3 meV for GaN and 21.7 meV for AlN, Ref. 16) is not included here.

For GaN, the HH(Γ_9) and LH(Γ_7) bands are highest in energy under compressive strain. Under tensile biaxial stress, the CF(Γ_7) band becomes the highest-lying valence band. This leads to a kink between the linear regions in the band-gap-versus-strain plot [Fig. 2(a)], consistent with experimental observations.[17] The variation of band gap with volume ($dE_g/d\ln V$) for biaxial stress is −10.90 eV for the energy gap between the CF(Γ_7) valence band and the conduction band, and −4.29 eV for the energy gap between the HH(Γ_9)/LH(Γ_7) valence band and the conduction band. In unstrained AlN, the highest energy band is the CF(Γ_7) band, and it remains the topmost valence band over the entire strain range explored here (Fig. 2(b)], consistent with experimental observations.[18] For AlN under biaxial stress, $dE_g/d\ln V = -15.76$ eV. Values of $dE_g/d\ln V$ calculated here are within 8% of the values derived from calculations in Ref. 9.

Figure 3 shows the variation of the electron effective mass with strain in GaN and AlN. For the case of hydrostatic stress, tensile strain causes the effective mass parallel and perpendicular to the c direction to decrease linearly in both GaN and AlN. The calculated variation of the effective mass with volume (i.e., under hydrostatic stress) for GaN, expressed as $d\ln m^*/d\ln V$, is −1.7 for $m_e^{\perp}$ and −1.8 for $m_e^{\parallel}$. These values are in good agreement with those calculated by Svane *et al.*[4] using the quasiparticle, self-consistent *GW* approach: −1.8 for $m_e^{\perp}$ and −1.9 for $m_e^{\parallel}$. For AlN, we find $d\ln m^*/d\ln V$ is −1.1 for $m_e^{\perp}$ and −1.2 for $m_e^{\parallel}$. For the case of biaxial stress, tensile strain causes $m_e^{\perp}$ in GaN and AlN to decrease at a similar rate as in the case of hydrostatic stress, while $m_e^{\parallel}$ *increases* with tensile strain.

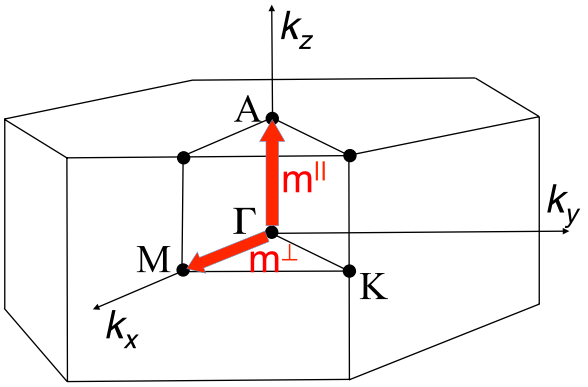

FIG. 1. Brillouin zone of the wurtzite structure indicating high-symmetry directions. Arrows denote directions along which effective mass were calculated.

We examine this unexpected variation of $m_e^{\parallel}$ with strain by employing the $\mathbf{k}\cdot\mathbf{p}$ formalism.[19,20] For wurtzite III-nitride materials, the $\mathbf{k}\cdot\mathbf{p}$ Hamiltonian is expanded in a basis set that includes the conduction band and three highest valence bands, resulting in an 8×8 Hamiltonian matrix. Under the quasi-cubic approximation and neglecting the effects of other bands and spin-orbit coupling, the electron effective mass in the $\mathbf{k}\cdot\mathbf{p}$ formalism can be expressed as[20]

$$\frac{m_0}{m_e^{\parallel}} \simeq 1 + \frac{E_{\parallel}}{E_g + \Delta_{cr}}, \tag{1}$$

and

$$\frac{m_0}{m_e^{\perp}} \simeq 1 + \frac{E_{\perp}}{E_g}, \tag{2}$$

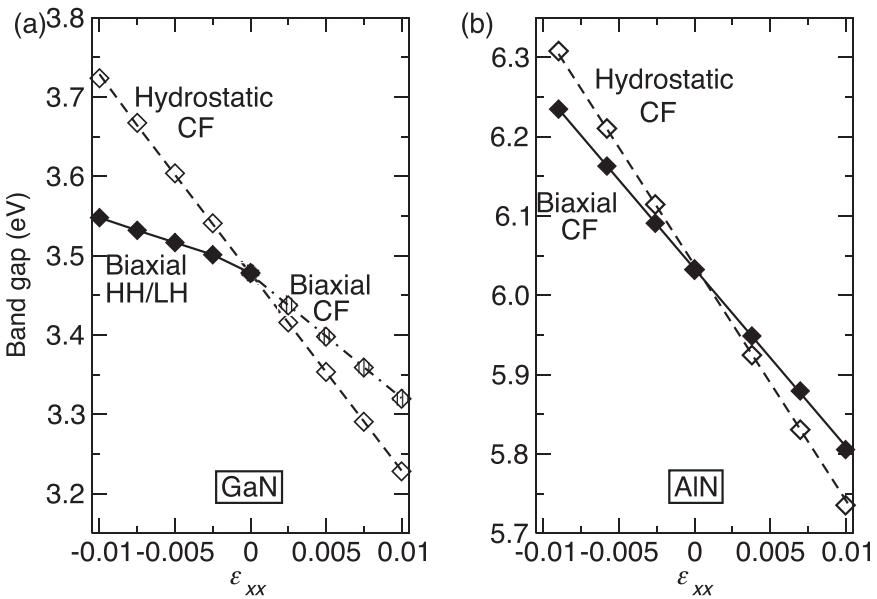

FIG. 2. Dependence of band gap on in-plane strain for (a) GaN and (b) AlN under hydrostatic and biaxial stresses. The topmost valence band is specified.

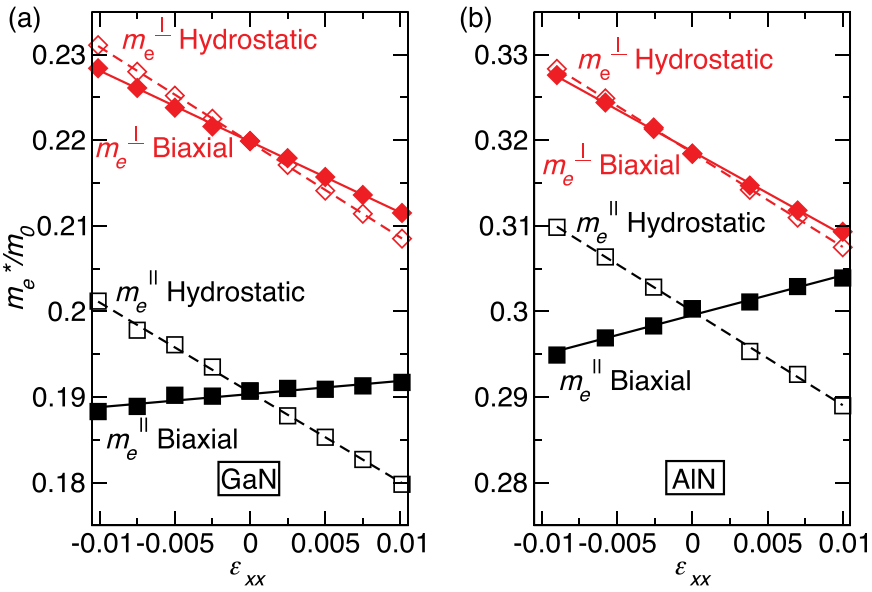

FIG. 3. Dependence of effective mass on in-plane strain for (a) GaN and (b) AlN, for hydrostatic as well as biaxial stress. The parallel ($m^{\parallel}$) and in-plane ($m^{\perp}$) directions are indicated in Fig. 1.

where $E_{\parallel}$ and $E_{\perp}$ are the so-called Kane parameters. These are related to the interband momentum matrix elements as follows: $E_{\parallel} = \frac{2}{m_0}|\langle CF|\hat{p}_{\parallel}|CB\rangle|^2$ and $E_{\perp} = \frac{2}{m_0}|\langle HH|\hat{p}_{\perp}|CB\rangle|^2 = \frac{2}{m_0}|\langle LH|\hat{p}_{\perp}|CB\rangle|^2$, where CB denotes the conduction band wave function.[21] This model is usually applied by fitting the Kane parameters to experimental or calculated data. Past applications of the model have assumed that the Kane parameters are constant, i.e., that they do not depend on strain. Here, we find that there is a distinct variation with strain, and we explicitly determine the parameters by calculating the momentum matrix elements between the wave functions for the conduction band and the three highest valence bands at different strains. The results are shown in Fig. 4.

In the case of hydrostatic stress, we find that the Kane parameters vary only slightly as a function of strain; therefore, according to Eqs. (1) and (2), the change in effective mass is dominated by the change in E_g, leading to the often-invoked trend that effective mass decreases with decreasing band gap (and thus with increasing hydrostatic stress, Fig. 3). In the case of biaxial stress, however, the Kane parameters change significantly with strain, with $E_{\parallel}$ and $E_{\perp}$ exhibiting opposite trends. This explains the opposite behavior in $m_e^{\parallel}$ and $m_e^{\perp}$ under biaxial stress, observed in Fig. 3. Therefore, for $\mathbf{k}\cdot\mathbf{p}$ to correctly capture the strain dependence of the effective mass in GaN and AlN, the effect of strain on the momentum matrix elements must be taken into account.

The calculated change in effective mass as a function of strain can be used to estimate the effect of strain on the electron mobility. For parabolic bands in the semiclassical model of conduction, the in-plane conductivity is given by[22]

$$\sigma_{\perp} = \frac{ne^2\tau}{m_e^{\perp}}, \tag{3}$$

where n is the number of carriers per unit volume and τ is the relaxation time, or the average time between scattering events. The electron mobility is given by the relaxation time divided by the effective mass. The in-plane mass, $m_e^{\perp}$, decreases with tensile strain at a rate of around 5% for a

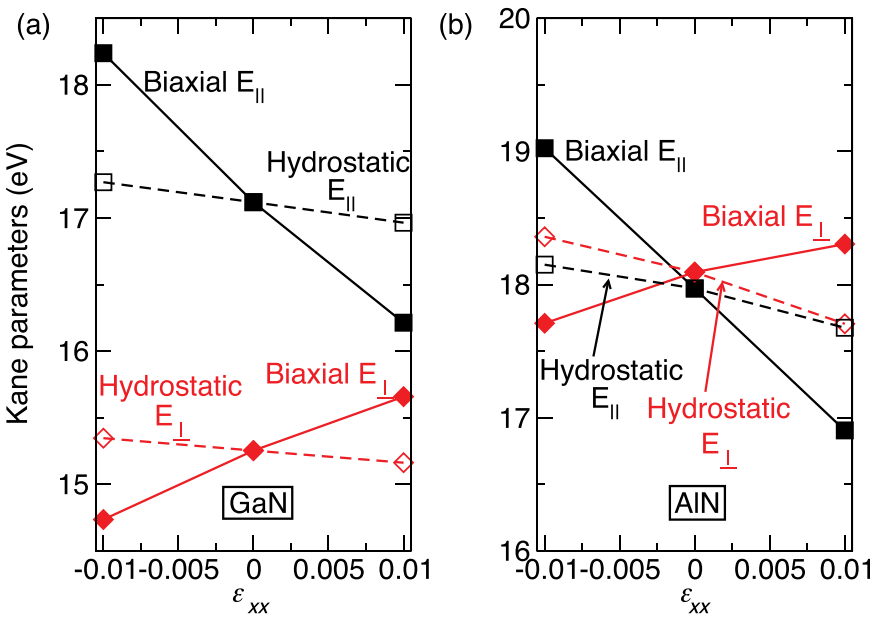

FIG. 4. Dependence of Kane parameters on strain for (a) GaN and (b) AlN under hydrostatic and biaxial stress.

strain of $\epsilon_{xx} = 0.01$. If all other variables in Eq. (3) are kept constant, this corresponds to an increase in mobility of less than 1%, over an order of magnitude too small to explain the increase in mobility reported in Ref. 2 based on measurements of strained HEMTs. The variation in effective mass with strain is clearly not the main contributor to the reported change in mobility. Such an enhancement, therefore, would require a substantial change in τ due to strain effects on scattering mechanisms in the two-dimensional electron gas. These effects are beyond the scope of the present study.

In conclusion, we have systematically studied the effect of strain on the effective mass of AlN and GaN using first-principles techniques based on hybrid density functional theory. Hydrostatic tensile stress causes a linear decrease of both $m_e^{\perp}$ and $m_e^{\parallel}$. Biaxial stress also results in a linearly decreasing $m_e^{\perp}$, but $m_e^{\parallel}$ increases linearly. An examination of the 8×8 $\mathbf{k} \cdot \mathbf{p}$ formalism shows that this behavior is caused by the strain dependence of the momentum matrix element between the valence and conduction bands, which is substantial for biaxial stress states. Our results show that the change of effective mass with stress cannot account for the changes in mobility reported in Ref. 2.

We thank T. Palacios for sharing his results, L. de Carvalho, A. Schleife, and F. Bechstedt for discussion of their results and help in calculating momentum matrix elements, and Q. Yan, D. Steiauf, A. Alkauskas, and H. Peelaers for helpful discussions. C.E.D. was supported by NSF (DMR-0906805) for first-principles calculations and by the Center for Energy Efficient Materials, an Energy Frontier Research Center funded by DOE, Office of Science, BES under Award Number DE-SC0001009 for the k.p theory analysis. Additional support was provided by the UCSB Solid State Lighting and Energy Center. Computational resources were provided by the Center for Scientific Computing at the CNSI and MRL (an NSF MRSEC, DMR-1121053) (NSF CNS-0960316), and the Extreme Science and Engineering Discovery Environment (XSEDE), and supported by NSF (OCI-1053575 and NSF DMR07-0072N).

[1]S. E. Thompson, S. Suthram, Y. Sun, G. Sun, S. Parthasarathy, M. Chu, and T. Nishida, "Future of strained Si/semiconductors in nanoscale MOSFETs," Tech. Dig.-IEDM **2006**, 1–4.
[2]M. Azize and T. Palacios, J. Appl. Phys. **108**, 023707 (2010).
[3]I. Gorczyca, J. Plesiewicz, L. Dmowski, T. Suski, N. E. Christensen, A. Svane, C. S. Gallinat, G. Koblmueller, and J. S. Speck, J. Appl. Phys. **104**, 013704 (2008).
[4]A. Svane, N. E. Christensen, I. Gorczyca, M. van Schilfgaarde, A. N. Chantis, and T. Kotani, Phys. Rev. B **82**, 115102 (2010).
[5]J. Heyd, G. E. Scuseria, and M. Ernzerhof, J. Chem. Phys. **118**, 8207 (2003).
[6]J. Heyd, G. E. Scuseria, and M. Ernzerhof, J. Chem. Phys. **124**, 219906 (2006).
[7]G. Kresse and J. Furthmüller, Phys. Rev. B **54**, 11169 (1996).
[8]P. E. Blöchl, Phys. Rev. B **50**, 17953 (1994).
[9]Q. Yan, P. Rinke, M. Scheffler, and C. G. Van de Walle, Appl. Phys. Lett. **95**, 121111 (2009).
[10]I. Vurgaftman and J. R. Meyer, J. Appl. Phys. **94**, 3675 (2003) and references therein.
[11]P. Rinke, M. Winkelnkemper, A. Qteish, D. Bimberg, J. Neugebauer, and M. Scheffler, Phys. Rev. B **77**, 075202 (2008).
[12]J. L. Lyons, A. Janotti, and C. G. Van de Walle, Appl. Phys. Lett. **97**, 152108 (2010).
[13]M. Ueno, M. Yoshida, A. Onodera, O. Shimomura, and K. Takemura, Phys. Rev. B **49**, 14 (1994).
[14]A. Janotti and C. G. Van de Walle, Phys. Rev. B **75**, 121201(R) (2007).
[15]G. D. Chen, M. Smith, J. Y. Lin, H. X. Jiang, S.-H. Wei, M. Asif Khan, and C. J. Sun, Appl. Phys. Lett. **68**, 2784 (1996).
[16]L. C. de Carvalho, A. Schleife, and F. Bechstedt, Phys. Rev. B **84**, 195105 (2011).
[17]A. Shikanai, T. Azuhata, T. Sota, S. Chichibu, A. Kuramata, K. Horino, and S. Nakamura, J. Appl. Phys. **81**, 417 (1997).
[18]H. Ikeda, T. Okamura, K. Matasukawa, T. Sota, M. Sugawara, T. Hoshi, P. Cantu, R. Sharma, J. F. Kaeding, S. Keller, U. K. Mishra, K. Kosaka, K. Asai, S. Sumiya, T. Shibata, M. Tanaka, J. S. Speck, S. P. DenBaars, S. Nakamura, T. Koyama, T. Onuma, and S. F. Chichibu, J. Appl. Phys. **102**, 123707 (2007).
[19]G. L. Bir and G. E. Pikus, *Symmetry and Strain-Induced Effects in Semiconductors* (Wiley, New York, 1974).
[20]S. L. Chuang and C. S. Chang, Phys. Rev. B **54**, 2491 (1996).
[21]E. O. Kane, J. Phys. Chem. Solids **1**, 249 (1957).
[22]N. W. Ashcroft and N. D. Mermin, *Solid State Physics* (Holt, Rinehart, and Winston, Pennsylvania, 1976), pp. 250 and 251.